

LEARNING HIGH-DIMENSIONAL DIRECTED ACYCLIC GRAPHS WITH LATENT AND SELECTION VARIABLES

BY DIEGO COLOMBO¹, MARLOES H. MAATHUIS¹, MARKUS
KALISCH AND THOMAS S. RICHARDSON²

ETH Zürich, ETH Zürich, ETH Zürich and University of Washington

We consider the problem of learning causal information between random variables in directed acyclic graphs (DAGs) when allowing arbitrarily many latent and selection variables. The FCI (Fast Causal Inference) algorithm has been explicitly designed to infer conditional independence and causal information in such settings. However, FCI is computationally infeasible for large graphs. We therefore propose the new RFCI algorithm, which is much faster than FCI. In some situations the output of RFCI is slightly less informative, in particular with respect to conditional independence information. However, we prove that any causal information in the output of RFCI is correct in the asymptotic limit. We also define a class of graphs on which the outputs of FCI and RFCI are identical. We prove consistency of FCI and RFCI in sparse high-dimensional settings, and demonstrate in simulations that the estimation performances of the algorithms are very similar. All software is implemented in the R-package `pcalg`.

1. Introduction. We consider the problem of learning the causal structure between random variables in acyclic systems with arbitrarily many latent and selection variables. As background information, we first discuss the situation without latent and selection variables in Section 1.1. Next, in Section 1.2 we discuss complications that arise when allowing for arbitrarily many latent and selection variables. Our new contributions are outlined in Section 1.3.

Received April 2011; revised August 2011.

¹Supported in part by Swiss NSF Grant 200021-129972.

²Supported in part by U.S. NSF Grant CRI 0855230 and U.S. NIH Grant R01 AI032475.

AMS 2000 subject classifications. Primary 62H12, 62M45, 62-04; secondary 68T30.

Key words and phrases. Causal structure learning, FCI algorithm, RFCI algorithm, maximal ancestral graphs (MAGs), partial ancestral graphs (PAGs), high-dimensionality, sparsity, consistency.

<p>This is an electronic reprint of the original article published by the Institute of Mathematical Statistics in <i>The Annals of Statistics</i>, 2012, Vol. 40, No. 1, 294–321. This reprint differs from the original in pagination and typographic detail.</p>
--

1.1. *Systems without latent and selection variables.* We first consider systems that satisfy the assumption of causal sufficiency, that is, that there are no unmeasured common causes and no unmeasured selection variables. We assume that causal information between variables can be represented by a directed acyclic graph (DAG) in which the vertices represent random variables and the edges represent direct causal effects (see, e.g., [13, 14, 20]). In particular, X_1 is a direct cause of X_2 only if $X_1 \rightarrow X_2$ (i.e., X_1 is a parent of X_2), and X_1 is a (possibly indirect) cause of X_2 only if there is a directed path from X_1 to X_2 (i.e., X_1 is an ancestor of X_2).

Each causal DAG implies a set of conditional independence relationships which can be read off from the DAG using a concept called d -separation [13]. Several DAGs can describe exactly the same conditional independence information. Such DAGs are called Markov equivalent and form a Markov equivalence class. For example, consider DAGs on the variables $\{X_1, X_2, X_3\}$. Then $X_1 \rightarrow X_2 \rightarrow X_3$, $X_1 \leftarrow X_2 \leftarrow X_3$ and $X_1 \leftarrow X_2 \rightarrow X_3$ form a Markov equivalence class, since they all imply the single conditional independence relationship $X_1 \perp\!\!\!\perp X_3 | X_2$, that is, X_1 is conditionally independent of X_3 given X_2 (using the shorthand notation of Dawid [7]). Another Markov equivalence class is given by the single DAG $X_1 \rightarrow X_2 \leftarrow X_3$, since this is the only DAG that implies the conditional independence relationship $X_1 \perp\!\!\!\perp X_3$ alone. Markov equivalence classes of DAGs can be described uniquely by a completed partially directed acyclic graph (CPDAG) [3, 4].

CPDAGs can be learned from conditional independence information if one assumes faithfulness, that is, if the conditional independence relationships among the variables are exactly equal to those that are implied by the DAG via d -separation. For example, suppose that the distribution of $\{X_1, X_2, X_3\}$ is faithful to an unknown underlying causal DAG, and that the only conditional independence relationship is $X_1 \perp\!\!\!\perp X_3 | X_2$. Then the corresponding Markov equivalence class consists of $X_1 \rightarrow X_2 \rightarrow X_3$, $X_1 \leftarrow X_2 \leftarrow X_3$ and $X_1 \leftarrow X_2 \rightarrow X_3$, and we know that one of these three DAGs must be the true causal DAG. Algorithms that are based on this idea are called constraint-based algorithms, and a prominent example is the PC algorithm [20]. The PC algorithm is sound (i.e., correct) and complete (i.e., maximally informative) under the assumptions of causal sufficiency and faithfulness [20]. It is efficiently implemented in the R-package `pcalg` [9], and was shown to be asymptotically consistent in sparse high-dimensional settings [8].

In practice, one often wants to estimate not only the Markov equivalence class of DAGs, but also the size of causal effects between pairs of variables. In the special case that the estimated CPDAG represents a single DAG, one can do this via, for example, Pearl's do-calculus (also called intervention calculus; see [13]) or marginal structural models [18]. If the estimated CPDAG represents several DAGs, one can conceptually estimate causal effects for each DAG in the Markov equivalence class, and use these values to infer

bounds on causal effects. This idea, together with a fast local implementation, forms the basis of the IDA algorithm [10, 11] which estimates bounds on causal effects from observational data that are generated from an unknown causal DAG (IDA stands for Intervention calculus when the DAG is Absent). The IDA algorithm was shown to be consistent in sparse high-dimensional settings [11], and was validated on a challenging high-dimensional yeast gene expression data set [10].

1.2. *Complications arising from latent and selection variables.* In practice there are often latent variables, that is, variables that are not measured or recorded. Statistically speaking, these variables are marginalized out. Moreover, there can be selection variables, that is, unmeasured variables that determine whether or not a measured unit is included in the data sample. Statistically speaking, these variables are conditioned on (see [6, 21] for a more detailed discussion). Latent and selection variables cause several complications.

The first problem is that causal inference based on the PC algorithm may be incorrect. For example, consider the DAG in Figure 1(a) with observed variables $\mathbf{X} = \{X_1, X_2, X_3\}$ and latent variables $\mathbf{L} = \{L_1, L_2\}$. The only conditional independence relationship among the observed variables is $X_1 \perp\!\!\!\perp X_3$. There is only one DAG on \mathbf{X} that implies this single conditional independence relationship, namely $X_1 \rightarrow X_2 \leftarrow X_3$, and this will therefore be the output of the PC algorithm; see Figure 1(b). This output would lead us to believe that both X_1 and X_3 are causes of X_2 . But this is clearly incorrect, since in the underlying DAG with latent variables, there is neither a directed path from X_1 to X_2 nor one from X_3 to X_2 .

A second problem is that the space of DAGs is not closed under marginalization and conditioning [16] in the following sense. If a distribution is faithful to a DAG, then the distribution obtained by marginalizing out and conditioning on some of the variables may *not* be faithful to any DAG on the observed variables. For example, consider the DAG $X_1 \rightarrow X_2 \leftarrow L_1 \rightarrow X_3 \leftarrow X_4$. This DAG implies the following set of conditional independence relationships among the observed variables $\mathbf{X} = \{X_1, \dots, X_4\}$: $X_1 \perp\!\!\!\perp X_3$, $X_1 \perp\!\!\!\perp X_4$,

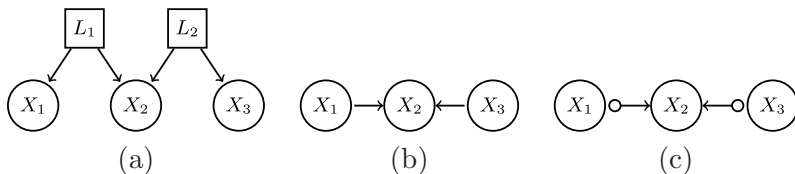


FIG. 1. Graphs corresponding to the examples in Section 1.2. Throughout we use square boxes to represent latent variables and circles to represent observed variables. (a) DAG with latent variables; (b) CPDAG; (c) PAG.

$X_2 \perp\!\!\!\perp X_4$, $X_1 \perp\!\!\!\perp X_3|X_4$, $X_1 \perp\!\!\!\perp X_4|X_2$, $X_1 \perp\!\!\!\perp X_4|X_3$ and $X_2 \perp\!\!\!\perp X_4|X_1$, and others implied by these. There is no DAG on \mathbf{X} that entails exactly this set of conditional independencies via d -separation.

These problems can be solved by introducing a new class of graphs on the observed variables, called maximal ancestral graphs (MAGs) [16]. Every DAG with latent and selection variables can be transformed into a unique MAG over the observed variables ([16], page 981). Several DAGs can lead to the same MAG. In fact, a MAG describes infinitely many DAGs since no restrictions are made on the number of latent and selection variables.

MAGs encode causal relationships between the observed variables via the edge marks. For example, consider the edge $X_1 \rightarrow X_2$ in a MAG. The tail at X_1 implies that X_1 is a cause (ancestor) of X_2 or of a selection variable, and the arrowhead at X_2 implies that X_2 is not a cause (not an ancestor) of X_1 nor of any selection variable, in all possible underlying DAGs with latent and selection variables. Moreover, MAGs encode conditional independence relationships among the observed variables via m -separation [16], a generalization of d -separation (see Definition 2.1 in Section 2.2). Several MAGs can describe exactly the same conditional independence relationships; see [2]. Such MAGs form a Markov equivalence class which can be represented by a partial ancestral graph (PAG); see Definition 3.1. PAGs describe causal features common to every MAG in the Markov equivalence class, and hence to every DAG (possibly with latent and selection variables) compatible with the observable independence structure under the assumption of faithfulness. For example, consider again the DAG in Figure 1(a). The only conditional independence relationship among the observed variables is $X_1 \perp\!\!\!\perp X_3$, and this is represented by the PAG in Figure 1(c). This PAG implies that X_2 is not a cause (ancestor) of X_1 , X_3 or a selection variable, and this is indeed the case in the underlying DAG in Figure 1(a) and is true of any DAG that, assuming faithfulness, could have implied $X_1 \perp\!\!\!\perp X_3$. The two circle marks at X_1 and X_3 in Figure 1(c) represent uncertainty about whether or not X_1 and X_3 are causes of X_2 . This reflects the fact that the single conditional independence relationship $X_1 \perp\!\!\!\perp X_3$ among the observed variables can arise from the DAG $X_1 \rightarrow X_2 \leftarrow X_3$ in which X_1 and X_3 are causes of X_2 , but it can also arise from the DAG in Figure 1(a) in which X_1 and X_3 are not causes of X_2 .

Under the faithfulness assumption, a Markov equivalence class of DAGs with latent and selection variables can be learned from conditional independence information among the observed variables alone using the Fast Causal Inference (FCI) algorithm [20], which is a modification of the PC algorithm. Originally, the output of FCI was defined as a partially oriented inducing path graph (POIPG), but its output can also be interpreted as a PAG [23]. Spirtes et al. [20] proved that the FCI algorithm is sound in the presence of arbitrarily many latent variables. Spirtes et al. [21] extended the soundness

proof to allow for selection variables as well. Zhang [24] recently introduced extra orientation rules that make FCI complete when its output is interpreted as a PAG. Despite its name, FCI is computationally very intensive for large graphs.

Spirites [19] introduced a modified version of FCI, called Anytime FCI, that only considers conditional independence tests with conditioning sets of size less than some prespecified cut-off K . Anytime FCI is typically faster but less informative than FCI, but the causal interpretation of tails and arrowheads in its output is still sound.

Some work on the estimation of the size of causal effects in situations with latent and selection variables can be found in [17, 23] and in Chapter 7 of [20].

1.3. *New contributions.* We introduce a new algorithm for learning PAGs, called the *Really Fast Causal Inference* (RFCI) algorithm (see Section 3.2). RFCI uses fewer conditional independence tests than FCI, and its tests condition on a smaller number of variables. As a result, RFCI is much faster than FCI and its output tends to be more reliable for small samples, since conditional independence tests of high order have low power. On the other hand, the output of RFCI may be less informative. In this sense, the algorithm is related to the Anytime FCI algorithm [19].

In Section 3.4 we compare the outputs of FCI and RFCI, and define a class of graphs for which the outputs of FCI and RFCI are identical.

In Section 4 we prove consistency of FCI and RFCI in sparse high-dimensional settings. The sparsity conditions needed for consistency of FCI are stronger than those for RFCI, due to the higher complexity of the FCI algorithm.

In order to compare RFCI to existing algorithms, we propose several small modifications of FCI and Anytime FCI. In particular, we introduce the Adaptive Anytime FCI (AAFCI) algorithm (see Section 3 of the supplementary document [5]) and we propose several ways to speed up the FCI and AAFCI algorithms (see Section 3.1).

We show in simulations (see Section 5) that the numbers of errors made by all algorithms are very similar. Moreover, we show that our modifications of FCI and AAFCI shorten the computation time considerably, but that for large graphs, RFCI is the only feasible algorithm.

All proofs, a description of AAFCI, pseudocodes and two additional examples are given in the supplementary document [5]. The R-package `pcalg` [9] contains implementations of all algorithms.

2. Preliminaries. This section introduces terminology that is used throughout the paper. Section 2.1 defines various graphical concepts, and Section 2.2 describes how graphs can be interpreted probabilistically and causally.

2.1. *Graphical definitions.* A graph $\mathcal{G} = (\mathbf{V}, \mathbf{E})$ is composed of a set of vertices $\mathbf{V} = \{X_1, \dots, X_p\}$ and a set of edges \mathbf{E} . In our framework, the vertices represent random variables and the edges describe conditional independence and ancestral relationships. The edge set \mathbf{E} can contain (a subset of) the following six types of edges: \rightarrow (*directed*), \leftrightarrow (*bi-directed*), $-$ (*undirected*), $\circ\text{--}\circ$ (*nondirected*), $\text{--}\circ$ (*partially undirected*) and $\circ\rightarrow$ (*partially directed*). The endpoints of an edge are called *marks* and they can be *tails*, *arrowheads* or *circles*. We use the symbol “*” to denote an arbitrary edge mark. A graph containing only directed edges is called *directed*, and one containing only undirected edges is called *undirected*. A *mixed* graph can contain directed, bi-directed and undirected edges. If we are only interested in the presence and absence of edges in a graph and not in the edge marks, we refer to the *skeleton* of the graph.

All the graphs we consider are *simple* in that there is at most one edge between any two vertices. If an edge is present, the vertices are said to be *adjacent*. If all pairs of vertices in a graph are adjacent, the graph is called *complete*. The *adjacency set* of a vertex X_i in a graph \mathcal{G} is the set of all vertices in $\mathbf{V} \setminus \{X_i\}$ that are adjacent to X_i in \mathcal{G} , denoted by $\text{adj}(\mathcal{G}, X_i)$. A vertex X_j in $\text{adj}(\mathcal{G}, X_i)$ is called a *parent* of X_i if $X_j \rightarrow X_i$, a *child* of X_i if $X_i \rightarrow X_j$, a *spouse* of X_i if $X_i \leftrightarrow X_j$, and a *neighbor* of X_i if $X_i - X_j$. The corresponding sets of parents, children, spouses and neighbors are denoted by $\text{pa}(\mathcal{G}, X_i)$, $\text{ch}(\mathcal{G}, X_i)$, $\text{sp}(\mathcal{G}, X_i)$ and $\text{ne}(\mathcal{G}, X_i)$, respectively.

A *path* is a sequence of distinct adjacent vertices. A path $\langle X_i, X_j, \dots, X_k \rangle$ is said to be *out of* (*into*) X_i if the edge between X_i and X_j has a tail (arrowhead) at X_i . A *directed path* is a path along directed edges that follows the direction of the arrowheads. A *cycle* occurs when there is a path from X_i to X_j and X_i and X_j are adjacent. A directed path from X_i to X_j forms a *directed cycle* together with the edge $X_j \rightarrow X_i$, and it forms an *almost directed cycle* together with the edge $X_j \leftrightarrow X_i$. If there is a directed path π from X_i to X_j or if $X_i = X_j$, the vertex X_i is called an *ancestor* of X_j and X_j a *descendant* of X_i . The sets of ancestors and descendants of a vertex X_i in \mathcal{G} are denoted by $\text{an}(\mathcal{G}, X_i)$ and $\text{de}(\mathcal{G}, X_i)$, respectively. These definitions are applied to a set $\mathbf{Y} \subseteq \mathbf{V}$ of distinct vertices as follows:

$$\begin{aligned} \text{an}(\mathcal{G}, \mathbf{Y}) &= \{X_i \mid X_i \in \text{an}(\mathcal{G}, X_j) \text{ for some } X_j \in \mathbf{Y}\}; \\ \text{de}(\mathcal{G}, \mathbf{Y}) &= \{X_i \mid X_i \in \text{de}(\mathcal{G}, X_j) \text{ for some } X_j \in \mathbf{Y}\}. \end{aligned}$$

Three vertices that form a cycle are called a *triangle*. Three vertices $\langle X_i, X_j, X_k \rangle$ are called an *unshielded triple* if X_i and X_j are adjacent, X_j and X_k are adjacent, but X_i and X_k are not adjacent. A nonendpoint vertex X_j on a path π is a *collider* on the path if both the edges preceding and succeeding it have an arrowhead at X_j , that is, if the path contains $*\rightarrow X_j \leftarrow *$. A nonendpoint vertex X_j on a path π which is not a collider is a *noncollider* on the path. An unshielded triple $\langle X_i, X_j, X_k \rangle$ is called a *v-structure* if X_j is a collider on the path $\langle X_i, X_j, X_k \rangle$.

A path $\pi = \langle X_l, \dots, X_j, X_b, X_p \rangle$ in a mixed graph is called a *discriminating path for X_b* if the following three conditions hold: (i) π includes at least three edges; (ii) X_b is a nonendpoint vertex on π and is adjacent to X_p on π ; and (iii) X_l is not adjacent to X_p in the graph and every vertex between X_l and X_b is a collider on π and a parent of X_p . An example of a discriminating path is given in Figure 4 of [5], where the circle marks are replaced by stars.

A graph $\mathcal{G} = (\mathbf{V}, \mathbf{E})$ is called *connected* if there exists a path between any pair of vertices in \mathbf{V} . A graph is called *biconnected* if it is connected and remains so if any vertex and its incident edges were to be removed. A *biconnected component* of a graph is a maximally biconnected subgraph [1].

A directed graph $\mathcal{G} = (\mathbf{V}, \mathbf{E})$ is called a *directed acyclic graph* (DAG) if it does not contain directed cycles. A mixed graph $\mathcal{G} = (\mathbf{V}, \mathbf{E})$ is called an *ancestral graph* if (i) it does not contain directed cycles, (ii) it does not contain almost directed cycles, and (iii) for any undirected edge $X_i - X_j$ in \mathbf{E} , X_i and X_j have no parents or spouses. DAGs form a subset of ancestral graphs.

2.2. *Probabilistic and causal interpretation of graphs.* A DAG entails conditional independence relationships via a graphical criterion called *d*-separation, which is a special case of *m*-separation:

DEFINITION 2.1 (Richardson and Spirtes [16]). A path π in an ancestral graph is said to be blocked by a set of vertices \mathbf{Y} if and only if:

- (i) π contains a subpath $\langle X_i, X_j, X_k \rangle$ such that the middle vertex X_j is a noncollider on this path and $X_j \in \mathbf{Y}$, or
- (ii) π contains a v-structure $X_i \ast \rightarrow X_j \leftarrow \ast X_k$ such that $X_j \notin \mathbf{Y}$ and no descendant of X_j is in \mathbf{Y} .

Vertices Z and W are *m*-separated by \mathbf{Y} if every path π between Z and W is blocked by \mathbf{Y} . Sets of vertices \mathbf{Z} and \mathbf{W} are *m*-separated by \mathbf{Y} if all pairs of vertices $Z \in \mathbf{Z}$, $W \in \mathbf{W}$ are *m*-separated by \mathbf{Y} .

If two vertices X_i and X_j in a DAG \mathcal{G} are *d*-separated by a subset \mathbf{Y} of the remaining vertices, then $X_i \perp\!\!\!\perp X_j | \mathbf{Y}$ in any distribution Q that factorizes according to \mathcal{G} (i.e., the joint density can be written as the product of the conditional densities of each variable given its parents in \mathcal{G} : $q(X_1, \dots, X_p) = \prod_{i=1}^p q(X_i | \text{pa}(\mathcal{G}, X_i))$). A distribution Q is said to be *faithful* to a DAG \mathcal{G} if the reverse implication also holds, that is, if the conditional independence relationships in Q are exactly the same as those that can be inferred from \mathcal{G} using *d*-separation. A set \mathbf{Y} that *d*-separates X_i and X_j in a DAG is called a *minimal separating set* if no subset of \mathbf{Y} *d*-separates X_i and X_j . A set \mathbf{Y} is a *minimal separating set for X_i and X_j given \mathbf{S}* if X_i and X_j are *d*-separated by $\mathbf{Y} \cup \mathbf{S}$ and there is no subset \mathbf{Y}' of \mathbf{Y} such that X_i and X_j are *d*-separated by $\mathbf{Y}' \cup \mathbf{S}$.

When a DAG $\mathcal{G} = (\mathbf{V}, \mathbf{E})$ contains latent and selection variables, we write $\mathbf{V} = \mathbf{X} \dot{\cup} \mathbf{L} \dot{\cup} \mathbf{S}$, where \mathbf{X} represents the observed variables, \mathbf{L} represents the latent variables and \mathbf{S} represents the selection variables, and these sets are disjoint (i.e., $\dot{\cup}$ denotes the union of disjoint sets).

A *maximal ancestral graph* (MAG) is an ancestral graph in which every missing edge corresponds to a conditional independence relationship. Richardson and Spirtes ([16], page 981) give an algorithm to transform a DAG $\mathcal{G} = (\mathbf{X} \dot{\cup} \mathbf{L} \dot{\cup} \mathbf{S}, \mathbf{E})$ into a unique MAG \mathcal{G}^* as follows. Let \mathcal{G}^* have vertex set \mathbf{X} . For any pair of vertices $X_i, X_j \in \mathbf{X}$ make them adjacent in \mathcal{G}^* if and only if there is an inducing path (see Definition 3.5) between X_i and X_j in \mathcal{G} relative to \mathbf{X} given \mathbf{S} . Moreover, for each edge $X_i \ast\ast X_j$ in \mathcal{G}^* put an arrowhead at X_i if $X_i \notin \text{an}(\mathcal{G}, \{X_j\} \cup \mathbf{S})$ and put a tail otherwise. The resulting MAG $\mathcal{G}^* = (\mathbf{X}, \mathbf{E}^*)$ encodes the conditional independence relationships holding in \mathcal{G} among the observed variables \mathbf{X} conditional on some value for the selection variables $\mathbf{S} = \mathbf{s}$; thus if X_i and X_j are m -separated by \mathbf{Y} in \mathcal{G}^* , then X_i and X_j are d -separated by $\mathbf{Y} \cup \mathbf{S}$ in \mathcal{G} and hence $X_i \perp\!\!\!\perp X_j | (\mathbf{Y} \cup \{\mathbf{S} = \mathbf{s}\})$ in any distribution Q factorizing according to \mathcal{G} . Perhaps more importantly, an ancestral graph preserves the ancestral relationships encoded in the DAG.

Throughout the remainder of this paper, \mathbf{S} refers to either the set of variables \mathbf{S} or the event $\mathbf{S} = \mathbf{s}$, depending on the context.

3. Oracle versions of the algorithms. We consider the following problem: assuming that the distribution of $\mathbf{V} = \mathbf{X} \dot{\cup} \mathbf{L} \dot{\cup} \mathbf{S}$ is faithful to an unknown underlying causal DAG $\mathcal{G} = (\mathbf{V}, \mathbf{E})$, and given oracle information about all conditional independence relationships between pairs of variables X_i and X_j in \mathbf{X} given sets $\mathbf{Y} \cup \mathbf{S}$ where $\mathbf{Y} \subseteq \mathbf{X} \setminus \{X_i, X_j\}$, we want to infer information about the ancestral (causal) relationships of the variables in the underlying DAG, which we represent via a PAG.

We discuss and compare two algorithms for this purpose, the FCI algorithm and our new RFCI algorithm. We first define the outputs of both algorithms: an FCI-PAG and an RFCI-PAG. (An FCI-PAG is usually referred to simply as a ‘‘PAG,’’ but in the remainder of this paper we use the name FCI-PAG to make a clear distinction between the output of the two algorithms.)

DEFINITION 3.1. Let \mathcal{G} be a DAG with partitioned vertex set $\mathbf{X} \dot{\cup} \mathbf{L} \dot{\cup} \mathbf{S}$. Let \mathcal{C} be a simple graph with vertex set \mathbf{X} and edges of the type $\rightarrow, \circ\rightarrow, \circ\circ, \leftrightarrow, -$ or $\circ-$. Then \mathcal{C} is said to be an FCI-PAG that represents \mathcal{G} if and only if, for any distribution P of $\mathbf{X} \dot{\cup} \mathbf{L} \dot{\cup} \mathbf{S}$ that is faithful to \mathcal{G} , the following four conditions hold:

- (i) the absence of an edge between two vertices X_i and X_j in \mathcal{C} implies that there exists a subset $\mathbf{Y} \subseteq \mathbf{X} \setminus \{X_i, X_j\}$ such that $X_i \perp\!\!\!\perp X_j | (\mathbf{Y} \cup \mathbf{S})$ in P ;

- (ii) the presence of an edge between two vertices X_i and X_j in \mathcal{C} implies that $X_i \not\perp\!\!\!\perp X_j | (\mathbf{Y} \cup \mathbf{S})$ in P for all subsets $\mathbf{Y} \subseteq \mathbf{X} \setminus \{X_i, X_j\}$;
- (iii) if an edge between X_i and X_j in \mathcal{C} has an arrowhead at X_j , then $X_j \notin \text{an}(\mathcal{G}, X_i \cup \mathbf{S})$;
- (iv) if an edge between X_i and X_j in \mathcal{C} has a tail at X_j , then $X_j \in \text{an}(\mathcal{G}, X_i \cup \mathbf{S})$.

DEFINITION 3.2. Let \mathcal{G} be a DAG with partitioned vertex set $\mathbf{X} \dot{\cup} \mathbf{L} \dot{\cup} \mathbf{S}$. Let \mathcal{C} be a simple graph with vertex set \mathbf{X} and edges of the type \rightarrow , $\circ\rightarrow$, $\circ\circ$, \leftrightarrow , $-$, or $\circ-$. Then \mathcal{C} is said to be an RFCI-PAG that represents \mathcal{G} if and only if, for any distribution P of $\mathbf{X} \dot{\cup} \mathbf{L} \dot{\cup} \mathbf{S}$ that is faithful to \mathcal{G} , conditions (i), (iii) and (iv) of Definition 3.1 and the following condition hold:

- (ii') the presence of an edge between two vertices X_i and X_j in \mathcal{C} implies that $X_i \not\perp\!\!\!\perp X_j | (\mathbf{Y} \cup \mathbf{S})$ for all subsets $\mathbf{Y} \subseteq \text{adj}(\mathcal{C}, X_i) \setminus \{X_j\}$ and for all subsets $\mathbf{Y} \subseteq \text{adj}(\mathcal{C}, X_j) \setminus \{X_i\}$.

Condition (ii) in Definition 3.1 is stronger than condition (ii') in Definition 3.2. Hence, the presence of an edge in an RFCI-PAG has a weaker interpretation than in an FCI-PAG. This has several consequences. First, every FCI-PAG is an RFCI-PAG. Second, different RFCI-PAGs for the same underlying DAG may have different skeletons, while the FCI-PAG skeleton is unique. In general, the RFCI-PAG skeleton is a supergraph of the FCI-PAG skeleton. Finally, an RFCI-PAG can correspond to more than one Markov equivalence class of DAGs (see Example 2 in Section 3.3).

It is worth noting that every FCI-PAG is an RFCI-PAG. Moreover, for a given pair of a graph \mathcal{G} and a distribution P faithful to it, there may be two different FCI-PAGs that represent \mathcal{G} but they will have the same skeleton. On the other hand, for a given pair of a graph \mathcal{G} and a distribution P faithful to it, there may also be more than one RFCI-PAG that represents \mathcal{G} and these different RFCI-PAGs can also have different skeletons.

The remainder of this section is organized as follows. Section 3.1 briefly discusses the FCI algorithm and proposes modifications that can speed up the algorithm while remaining sound and complete. Section 3.2 introduces our new RFCI algorithm. Section 3.3 discusses several examples that illustrate the commonalities and differences between the two algorithms, and Section 3.4 defines a class of graphs for which the outputs of FCI and RFCI are identical.

3.1. The FCI algorithm. A high-level sketch of FCI ([20], pages 144 and 145) is given in Algorithm 3.1. The sub-algorithms 4.1–4.3 are given in [5].

The determination of adjacencies in the PAG within the FCI algorithm is based on the following fact: if X_i is not an ancestor of X_j , and X_i and X_j are conditionally independent given some set $\mathbf{Y} \cup \mathbf{S}$ where $\mathbf{Y} \subseteq \mathbf{X} \setminus \{X_i, X_j\}$,

Algorithm 3.1 The FCI algorithm**Require:** Conditional independence information among all variables in \mathbf{X} given \mathbf{S}

- 1: Use Algorithm 4.1 of [5] to find an initial skeleton (\mathcal{C}), separation sets (sepset) and unshielded triple list (\mathfrak{M});
- 2: Use Algorithm 4.2 of [5] to orient v-structures (update \mathcal{C});
- 3: Use Algorithm 4.3 of [5] to find the final skeleton (update \mathcal{C} and sepset);
- 4: Use Algorithm 4.2 of [5] to orient v-structures (update \mathcal{C});
- 5: Use rules (R1)–(R10) of [24] to orient as many edge marks as possible (update \mathcal{C});
- 6: **return** \mathcal{C} , sepset.

then X_i and X_j are conditionally independent given $\mathbf{Y}' \cup \mathbf{S}$ for some subset \mathbf{Y}' of a certain set $\text{D-SEP}(X_i, X_j)$ or of $\text{D-SEP}(X_j, X_i)$ (see [20], page 134 for a definition). This means that, in order to determine whether there is an edge between X_i and X_j in an FCI-PAG, one does not need to test whether $X_i \perp\!\!\!\perp X_j | (\mathbf{Y} \cup \mathbf{S})$ for all possible subsets $\mathbf{Y} \subseteq \mathbf{X} \setminus \{X_i, X_j\}$, but only for all possible subsets $\mathbf{Y} \subseteq \text{D-SEP}(X_i, X_j)$ and $\mathbf{Y} \subseteq \text{D-SEP}(X_j, X_i)$. Since the sets $\text{D-SEP}(X_i, X_j)$ cannot be inferred from the observed conditional independencies, Spirtes et al. [20] defined a superset, called Possible-D-SEP, that can be computed:

DEFINITION 3.3. Let \mathcal{C} be a graph with any of the following edge types: $\circ\circ$, $\circ\rightarrow$, \leftrightarrow . *Possible-D-SEP*(X_i, X_j) in \mathcal{C} , denoted in shorthand by $\text{pds}(\mathcal{C}, X_i, X_j)$, is defined as follows: $X_k \in \text{pds}(\mathcal{C}, X_i, X_j)$ if and only if there is a path π between X_i and X_k in \mathcal{C} such that for every subpath $\langle X_m, X_l, X_h \rangle$ of π , X_l is a collider on the subpath in \mathcal{C} or $\langle X_m, X_l, X_h \rangle$ is a triangle in \mathcal{C} .

REMARK 3.1. Note that X_j does not play a role in the definition of $\text{pds}(\mathcal{C}, X_i, X_j)$, but we keep it as an argument because we will later consider alternative definitions of Possible-D-SEP (see Definition 3.4) where the second vertex X_j does play a role.

Since the definition of Possible-D-SEP requires some knowledge about the skeleton and orientation of edges, the FCI algorithm first finds an initial skeleton denoted by \mathcal{C}_1 in Step 1. This is done as in the PC-algorithm, by starting with a complete graph with edges $\circ\circ$ and performing conditional independence tests given subsets of increasing size of the adjacency sets of the vertices. An edge between X_i and X_j is deleted if a conditional independence is found, and the set responsible for this conditional independence is saved in $\text{sepset}(X_i, X_j)$ and $\text{sepset}(X_j, X_i)$ (see Algorithm 4.1 of [5]). The skeleton after completion of Step 1 is a superset of the final skeleton.

In Step 2, the algorithm orients unshielded triples $X_i * \circ X_j \circ * X_k$ as v-structures $X_i * \rightarrow X_j \leftarrow * X_k$ if and only if X_j is not in $\text{sepset}(X_i, X_k)$ and $\text{sepset}(X_k, X_i)$ (see Algorithm 4.2 of [5]).

The graph resulting after Step 2, denoted by \mathcal{C}_2 , contains sufficient information to compute the Possible-D-SEP sets. Thus, in Step 3, the algo-

rithm computes $\text{pds}(\mathcal{C}_2, X_i, \cdot)$ for every $X_i \in \mathbf{X}$. Then for every element X_j in $\text{adj}(\mathcal{C}_2, X_i)$, the algorithm tests whether $X_i \perp\!\!\!\perp X_j \mid (\mathbf{Y} \cup \mathbf{S})$ for every subset \mathbf{Y} of $\text{pds}(\mathcal{C}_2, X_i, \cdot) \setminus \{X_i, X_j\}$ and of $\text{pds}(\mathcal{C}_2, X_j, \cdot) \setminus \{X_j, X_i\}$ (see Algorithm 4.3 of [5]). As in Step 1, the tests are arranged in a hierarchical way starting with conditioning sets of small size. If there exists a set \mathbf{Y} that makes X_i and X_j conditionally independent given $\mathbf{Y} \cup \mathbf{S}$, the edge between X_i and X_j is removed and the set \mathbf{Y} is saved as the separation set in $\text{sepset}(X_i, X_j)$ and $\text{sepset}(X_j, X_i)$. After all conditional independence tests are completed, every edge in \mathcal{C} is reoriented as $\circ\text{--}\circ$, since the orientation of v-structures in Step 2 of the algorithm cannot necessarily be interpreted as specified in conditions (iii) and (iv) of Definition 3.1.

In Step 4, the v-structures are therefore oriented again based on the updated skeleton and the updated information in sepset (see Algorithm 4.2 of [5]). Finally, in Step 5 the algorithm replaces as many circles as possible by arrowheads and tails using the orientation rules described by [24].

First proposed modification: FCI_{path} . For sparse graphs, Step 3 of the FCI algorithm dramatically increases the computational complexity of the algorithm when compared to the PC algorithm. The additional computational effort can be divided in two parts: computing the Possible-D-SEP sets, and testing conditional independence given all subsets of these sets. The latter part is computationally infeasible when the sets $\text{pds}(\mathcal{C}_2, X_i, \cdot)$ are large, containing, say, more than 30 vertices. Since the size of the Possible-D-SEP sets plays such an important role in the complexity of the FCI algorithm, and since one has some freedom in defining these sets (they simply must be supersets of the D-SEP sets), we first propose a modification of the definition of Possible-D-SEP that can decrease its size.

DEFINITION 3.4. Let \mathcal{C} be a graph with any of the following edge types: $\circ\text{--}\circ$, $\circ\text{--}\rightarrow$, \leftrightarrow . Then, for two vertices X_i and X_j adjacent in \mathcal{C} , $\text{pds}_{\text{path}}(\mathcal{C}, X_i, X_j)$ is defined as follows: $X_k \in \text{pds}_{\text{path}}(\mathcal{C}, X_i, X_j)$ if and only if (i) there is a path π between X_i and X_k in \mathcal{C} such that for every subpath $\langle X_m, X_l, X_h \rangle$ of π , X_l is a collider on the subpath in \mathcal{C} or $\langle X_m, X_l, X_h \rangle$ is a triangle in \mathcal{C} , and (ii) X_k lies on a path between X_i and X_j .

For any pair of adjacent vertices X_i and X_j in a graph \mathcal{C} , the set $\text{pds}_{\text{path}}(\mathcal{C}, X_i, X_j)$ can be computed easily by intersecting $\text{pds}(\mathcal{C}, X_i, \cdot)$ with the unique biconnected component in \mathcal{C} that contains the edge between X_i and X_j . Algorithm 4.3 of [5] can now be modified as follows. Before line 1, we compute all biconnected components of the graph \mathcal{C}_2 , where \mathcal{C}_2 is the graph resulting from Step 2 of the FCI algorithm. Then between lines 3 and 4, we compute $\text{pds}_{\text{path}}(\mathcal{C}_2, X_i, X_j)$ as described above. Finally, on lines 8, 13 and 14, we replace $\text{pds}(\mathcal{C}_2, X_i, \cdot)$ by $\text{pds}_{\text{path}}(\mathcal{C}_2, X_i, X_j)$. We refer to the FCI algorithm with this modified version of Algorithm 4.3 of [5] as FCI_{path} .

Second class of modifications: CFCI, CFCI_{path}, SCFCI and SCFCI_{path}. Another possibility to decrease the size of Possible-D-SEP is to use conservative rules to orient v-structures in Step 2 of the FCI algorithm, so that fewer arrowheads are introduced, similarly to the Conservative PC algorithm [15]. This is especially helpful in the sample version of the algorithm (see Section 4.1), as the sample version tends to orient too many v-structures, which can lead to long chains of bi-directed edges and hence large Possible-D-SEP sets (see Figure 6 in Section 5.3).

The conservative orientation works as follows. For all unshielded triples $\langle X_i, X_j, X_k \rangle$ in \mathcal{C}_1 , where \mathcal{C}_1 is the graph resulting from Step 1 of the FCI algorithm, we determine all subsets \mathbf{Y} of $\text{adj}(\mathcal{C}_1, X_i)$ and of $\text{adj}(\mathcal{C}_1, X_k)$ satisfying $X_i \perp\!\!\!\perp X_k | (\mathbf{Y} \cup \mathbf{S})$. We refer to these sets as separating sets, and we label the triple $\langle X_i, X_j, X_k \rangle$ as *unambiguous* if and only if (i) at least one separating set \mathbf{Y} is found and either X_j is in all separating sets and in $\text{sepset}(X_i, X_k)$ or X_j is in none of the separating sets nor in $\text{sepset}(X_i, X_k)$, or (ii) no such separating set \mathbf{Y} is found. [Condition (ii) can occur, since separating sets found in Step 1 of the FCI algorithm do not need to be a subset of $\text{adj}(\mathcal{C}_1, X_i)$ or of $\text{adj}(\mathcal{C}_1, X_k)$.] At the end of Step 2, we only orient unambiguous triples satisfying $X_j \notin \text{sepset}(X_i, X_k)$ as v-structures. This may lead to different Possible-D-SEP sets in Step 3 (even in the oracle version of the algorithm), but other than that, Steps 3–5 of the algorithm remain unchanged. We refer to this version of the FCI algorithm as Conservative FCI (CFCI). If CFCI is used in combination with pds_{path} , we use the name CFCI_{path}.

Finally, the idea of conservative v-structures can also be applied in Step 4 of the FCI algorithm. For each unshielded triple $\langle X_i, X_j, X_k \rangle$ in \mathcal{C}_3 , where \mathcal{C}_3 is the graph resulting from Step 3, we determine all subsets \mathbf{Y} of $\text{adj}(\mathcal{C}_3, X_i)$ and of $\text{adj}(\mathcal{C}_3, X_k)$ satisfying $X_i \perp\!\!\!\perp X_k | (\mathbf{Y} \cup \mathbf{S})$. We then determine if a triple is unambiguous, and only if this is the case we orient it as v-structure or non-v-structure. Moreover, the orientation rules in Step 5 of the algorithm are adapted so that they only rely on unambiguous triples. We use the name Superconservative FCI (SCFCI) to refer to the version of FCI that uses conservative v-structures in both Steps 2 and 4. If SCFCI is used in combination with pds_{path} , we use the name SCFCI_{path}. The proof of Theorem 3.1 shows that the output of the oracle version of SCFCI is identical to that of CFCI. We still consider this version, however, in the hope to obtain better edge orientations in the sample versions of the algorithms, where the outputs are typically not identical.

Soundness of FCI follows from Theorem 5 of [21]. Soundness results for the modifications FCI_{path}, CFCI, CFCI_{path}, SCFCI and SCFCI_{path} are given in the following theorem:

THEOREM 3.1. *Consider one of the oracle versions of FCI_{path}, CFCI, CFCI_{path}, SCFCI or SCFCI_{path}. Let the distribution of $\mathbf{V} = \mathbf{X} \dot{\cup} \mathbf{L} \dot{\cup} \mathbf{S}$ be*

faithful to a DAG \mathcal{G} and let conditional independence information among all variables in \mathbf{X} given \mathbf{S} be the input to the algorithm. Then the output of the algorithm is an FCI-PAG of \mathcal{G} .

Completeness of FCI was proved by [24]. This means that the output of FCI is maximally informative, in the sense that for every circle mark there exists at least one MAG in the Markov equivalence class represented by the PAG where the mark is oriented as a tail, and at least one where it is oriented as an arrowhead. Completeness results of FCI_{path} , CFCI, $\text{CFCI}_{\text{path}}$, SCFCI and $\text{SCFCI}_{\text{path}}$ follow directly from the fact that, in the oracle versions, the orientation rules of these modifications boil down to the orientation rules of FCI.

3.2. The RFCI algorithm. The Really Fast Causal Inference (RFCI) algorithm is a modification of FCI. The main difference is that RFCI avoids the conditional independence tests given subsets of Possible-D-SEP sets, which can become very large even for sparse graphs. Instead, RFCI performs some additional tests before orienting v-structures and discriminating paths in order to ensure soundness, based on Lemmas 3.1 and 3.2 below. The number of these additional tests and the size of their conditioning sets is small for sparse graphs, since RFCI only conditions on subsets of the adjacency sets. As a result, RFCI is much faster than FCI for sparse graphs (see Section 5.3). Moreover, the lower computational complexity of RFCI leads to high-dimensional consistency results under weaker conditions than FCI [compare conditions (A3) and (A3') in Sections 4.2 and 4.3]. A high-level sketch of RFCI is given in Algorithm 3.2.

Step 1 of the algorithm is identical to Step 1 of Algorithm 3.1, and is used to find an initial skeleton \mathcal{C}_1 that satisfies conditions (i) and (ii') of Definition 3.2.

In Step 2 of the algorithm, unshielded triples are oriented based on Lemma 3.1 and some further edges may be removed.

LEMMA 3.1 (Unshielded triple rule). *Let the distribution of $\mathbf{V} = \mathbf{X} \dot{\cup} \mathbf{L} \dot{\cup} \mathbf{S}$ be faithful to a DAG \mathcal{G} . Assume that (a1) \mathbf{S}_{i_k} is a minimal separating set*

Algorithm 3.2 The RFCI algorithm

Require: Conditional independence information among all variables in \mathbf{X} given \mathbf{S}

- 1: Use Algorithm 4.1 of [5] to find an initial skeleton (\mathcal{C}), separation sets (sepset) and unshielded triple list (\mathfrak{M});
 - 2: Use Algorithm 4.4 of [5] to orient v-structures (update \mathcal{C} and sepset);
 - 3: Use Algorithm 4.5 of [5] to orient as many edge marks as possible (update \mathcal{C} and sepset);
 - 4: **return** \mathcal{C} , sepset.
-

for X_i and X_k given \mathbf{S} , and (a2) X_i and X_j as well as X_j and X_k are conditionally dependent given $(\mathbf{S}_{ik} \setminus \{X_j\}) \cup \mathbf{S}$. Then $X_j \in \text{an}(\mathcal{G}, \{X_i, X_k\} \cup \mathbf{S})$ if and only if $X_j \in \mathbf{S}_{ik}$.

The details of Step 2 are given in Algorithm 4.4 of [5]. We start with a list \mathfrak{M} of all unshielded triples in \mathcal{C}_1 , where \mathcal{C}_1 is the graph resulting from Step 1 of the RFCI algorithm, and an empty list \mathfrak{L} that is used to store triples that were found to satisfy the conditions of Lemma 3.1. For each triple $\langle X_i, X_j, X_k \rangle$ in \mathfrak{M} , we check if both X_i and X_j and X_j and X_k are conditionally dependent given $(\text{sepsset}(X_i, X_k) \setminus \{X_j\}) \cup \mathbf{S}$. These conditional dependencies may not have been checked in Step 1 of the algorithm, since $\text{sepsset}(X_i, X_k) \setminus \{X_j\}$ does not need to be a subset of $\text{adj}(\mathcal{C}_1, X_j)$. If both conditional dependencies hold, the triple satisfies the conditions of Lemma 3.1 and is added to \mathfrak{L} . On the other hand, an additional conditional independence relationship may be detected, say $X_i \perp\!\!\!\perp X_j | ((\text{sepsset}(X_i, X_k) \setminus \{X_j\}) \cup \mathbf{S})$. This may arise in a situation where X_i and X_j are not m -separated given a subset of vertices adjacent to X_i , and are not m -separated given a subset of vertices adjacent to X_j , but they do happen to be m -separated given the set $(\text{sepsset}(X_i, X_k) \setminus \{X_j\}) \cup \mathbf{S}$. In this situation, we remove the edge $X_i \ast\ast X_j$ from the graph, in agreement with condition (i) of Definition 3.2. The removal of this edge can create new unshielded triples, which are added to \mathfrak{M} . Moreover, it can destroy unshielded triples in \mathfrak{L} and \mathfrak{M} , which are therefore removed. Finally, by testing subsets of the conditioning set which led to removal of the edge, we find a *minimal* separating set for X_i and X_j and store it in $\text{sepsset}(X_i, X_j)$ and $\text{sepsset}(X_j, X_i)$. Example 1 of [5] shows that it is not sufficient to simply store $\text{sepsset}(X_i, X_k) \setminus \{X_j\}$ since it may not be minimal for X_i and X_j . We work with the lists \mathfrak{M} and \mathfrak{L} to ensure that the result of Step 2 does not depend on the order in which the unshielded triples are considered.

After Step 2, all unshielded triples still present in the graph are correctly oriented as a v-structure or non-v-structure. In Step 3, the algorithm orients as many further edges as possible, as described in Algorithm 4.5 of [5]. This procedure consists of repeated applications of the orientation rules (R1)–(R10) of [24], with the difference that rule (R4) about the discriminating path has been modified according to Lemma 3.2.

LEMMA 3.2 (Discriminating path rule). *Let the distribution of $\mathbf{V} = \mathbf{X} \dot{\cup} \mathbf{L} \dot{\cup} \mathbf{S}$ be faithful to a DAG \mathcal{G} . Let $\pi_{ik} = \langle X_i, \dots, X_l, X_j, X_k \rangle$ be a sequence of at least four vertices that satisfy: (a1) X_i and X_k are conditionally independent given $\mathbf{S}_{ik} \cup \mathbf{S}$, (a2) any two successive vertices X_h and X_{h+1} on π_{ik} are conditionally dependent given $(\mathbf{Y}' \setminus \{X_h, X_{h+1}\}) \cup \mathbf{S}$ for all $\mathbf{Y}' \subseteq \mathbf{S}_{ik}$, (a3) all vertices X_h between X_i and X_j (not including X_i and X_j) satisfy $X_h \in \text{an}(\mathcal{G}, X_k)$ and $X_h \notin \text{an}(\mathcal{G}, \{X_{h-1}, X_{h+1}\} \cup \mathbf{S})$, where X_{h-1} and X_{h+1}*

denote the vertices adjacent to X_h on π_{ik} . Then the following hold: (b1) if $X_j \in \mathbf{S}_{ik}$, then $X_j \in \text{an}(\mathcal{G}, \{X_k\} \cup \mathbf{S})$ and $X_k \notin \text{an}(\mathcal{G}, \{X_j\} \cup \mathbf{S})$, and (b2) if $X_j \notin \mathbf{S}_{ik}$, then $X_j \notin \text{an}(\mathcal{G}, \{X_l, X_k\} \cup \mathbf{S})$ and $X_k \notin \text{an}(\mathcal{G}, \{X_j\} \cup \mathbf{S})$.

Lemma 3.2 is applied as follows. For each triangle $\langle X_l, X_j, X_k \rangle$ of the form $X_j \circ \rightarrow X_k$, $X_j \ast \rightarrow X_l$ and $X_l \rightarrow X_k$, the algorithm searches for a discriminating path $\pi = \langle X_i, \dots, X_l, X_j, X_k \rangle$ for X_j of minimal length, and checks that the vertices in every consecutive pair (X_r, X_q) on π are conditionally dependent given $\mathbf{Y} \cup \mathbf{S}$ for all subsets \mathbf{Y} of $\text{sepset}(X_i, X_k) \setminus \{X_r, X_q\}$. (Example 2 of [5] shows why it is not sufficient to only check conditional dependence given $(\text{sepset}(X_i, X_k) \setminus \{X_r, X_q\}) \cup \mathbf{S}$, as we did for the v-structures.) If we do not find any conditional independence relationship, the path satisfies the conditions of Lemma 3.2 and is oriented as in rule (R4) of [24]. If one or more conditional independence relationships are found, the corresponding edges are removed, their minimal separating sets are stored, and any new unshielded triples that are created by removing the edges are oriented using Algorithm 4.4 of [5]. We note that the output of Step 3 may depend on the order in which the discriminating paths are considered.

Soundness of RFCI is stated in the following theorem.

THEOREM 3.2. *Let the distribution of $\mathbf{V} = \mathbf{X} \dot{\cup} \mathbf{L} \dot{\cup} \mathbf{S}$ be faithful to a DAG \mathcal{G} and let conditional independence information among all variables in \mathbf{X} given \mathbf{S} be the input to the RFCI algorithm. Then the output of RFCI is an RFCI-PAG of \mathcal{G} .*

REMARK 3.2. The new orientation rules based on Lemmas 3.1 and 3.2 open possibilities for different modifications of the FCI algorithm. For example, one could replace $\text{pds}(\mathcal{C}, X_i, X_j)$ by $\text{pds}_k(\mathcal{C}, X_i, X_j)$, where a vertex X_l is in $\text{pds}_k(\mathcal{C}, X_i, X_j)$ if it is in $\text{pds}(\mathcal{C}, X_i, X_j)$ and there is a path between X_i and X_l containing no more than $k + 1$ vertices. This modification yields a skeleton that is typically a superset of the skeleton of the true FCI-PAG. In order to infer correct causal orientations based on this skeleton, one needs to use Algorithms 4.4 and 4.5 of [5] to determine the final orientations of the edges. The parameter k represents a trade-off between computing time and informativeness of the output, where $k = 1$ corresponds to the RFCI algorithm and $k = |\mathbf{X}| - 2$ corresponds to the FCI algorithm.

Another way to obtain a more informative but slower version of RFCI can be obtained by modifying Step 1 of the RFCI algorithm: instead of considering all subsets of $\text{adj}(\mathcal{C}, X_i)$ and of $\text{adj}(\mathcal{C}, X_j)$, one can consider all subsets of the union $\text{adj}(\mathcal{C}, X_i) \cup \text{adj}(\mathcal{C}, X_j)$.

3.3. Examples. We now illustrate the algorithms in two examples. In Example 1, the outputs of FCI and RFCI are identical. In Example 2, the outputs of FCI and RFCI are not identical, and the output of RFCI describes two Markov equivalence classes. We will see, however, that the ancestral or

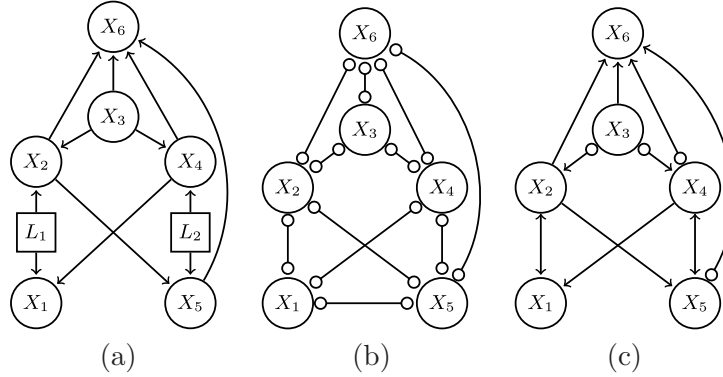


FIG. 2. Graphs corresponding to Example 1, where the outputs of FCI and RFCI are identical. (a) Underlying DAG with latent variables; (b) initial skeleton \mathcal{C}_1 ; (c) RFCI-PAG and FCI-PAG.

causal information inferred from an RFCI-PAG is correct. Two additional examples illustrating details of Algorithms 4.4 and 4.5 of [5] are given in Section 5 of [5].

EXAMPLE 1. Consider the DAG in Figure 2(a) containing observed variables $\mathbf{X} = \{X_1, \dots, X_6\}$, latent variables $\mathbf{L} = \{L_1, L_2\}$ and no selection variables ($\mathbf{S} = \emptyset$). Suppose that all conditional independence relationships over \mathbf{X} that can be read off from this DAG are used as input for the algorithms.

In all algorithms, Step 1 is the same, and consists of finding an initial skeleton. This skeleton, denoted by \mathcal{C}_1 , is shown in Figure 2(b). The final output given by both algorithms is shown in Figure 2(c).

Comparing the initial skeleton with the final skeleton, we see that the edge $X_1 \circ\!\!\!\circ X_5$ is present in the initial but not in the final skeleton. The absence in the final skeleton is due to the fact that $X_1 \perp\!\!\!\perp X_5 \mid \{X_2, X_3, X_4\}$. The edge is present in the initial skeleton, since this conditional independence is not found in Step 1 of the algorithms, because $\{X_2, X_3, X_4\}$ is not a subset of $\text{adj}(\mathcal{C}_1, X_1)$ nor of $\text{adj}(\mathcal{C}_1, X_5)$.

The FCI algorithm finds the conditional independence relationship $X_1 \perp\!\!\!\perp X_5 \mid \{X_2, X_3, X_4\}$ in Step 3 when subsets of Possible-D-SEP are considered, since $\text{pds}(\mathcal{C}_2, X_1, X_5) \setminus \{X_1, X_5\} = \{X_2, X_3, X_4\}$ and $\text{pds}(\mathcal{C}_2, X_5, X_1) \setminus \{X_5, X_1\} = \{X_2, X_3, X_4, X_6\}$, where \mathcal{C}_2 is the graph resulting from Step 2 of the algorithm.

In the RFCI algorithm, the conditional independence relationship $X_1 \perp\!\!\!\perp X_5 \mid \{X_2, X_3, X_4\}$ is also found, but by another mechanism. In Step 2 of Algorithm 3.2, unshielded triples are oriented after performing some additional conditional independence tests. In particular, when considering the triple $\langle X_1, X_5, X_6 \rangle$, the algorithm checks whether $X_1 \perp\!\!\!\perp X_5 \mid (\text{sepset}(X_1, X_6) \setminus \{X_5\})$, where $\text{sepset}(X_1, X_6) = \{X_2, X_3, X_4\}$.

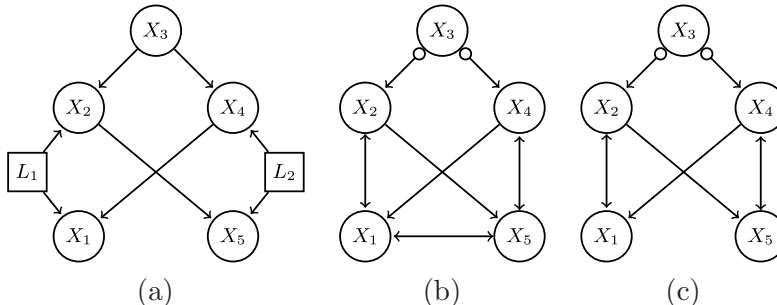


FIG. 3. Graphs corresponding to Example 2, where the outputs of FCI and RFCI are not identical. The output of RFCI corresponds to two Markov equivalence classes when interpreted as an RFCI-PAG. (a) Underlying DAG \mathcal{G} with latent variables; (b) output of RFCI for \mathcal{G} ; (c) output of FCI for \mathcal{G} .

This example also shows why it is necessary to check unshielded triples according to Lemma 3.1 before orienting them as v-structures. Omitting this check for triple $\langle X_1, X_5, X_6 \rangle$ would orient it as a v-structure, since $X_5 \notin \text{sepset}(X_1, X_6)$. Hence, we would conclude that $X_5 \notin \text{an}(\mathcal{G}, \{X_6\} \cup \mathbf{S})$, which contradicts the underlying DAG.

Finally, we see that the orientations of the edges are identical in the outputs of both algorithms, which implies that the outputs encode the same ancestral information.

EXAMPLE 2. Consider the DAG \mathcal{G} in Figure 3(a), containing observed variables $\mathbf{X} = \{X_1, \dots, X_5\}$, latent variables $\mathbf{L} = \{L_1, L_2\}$ and no selection variables ($\mathbf{S} = \emptyset$) (see also [21], page 228, Figure 8a). Suppose that all conditional independence relationships over \mathbf{X} that can be read off from this DAG are used as input for the algorithms.

The outputs of the RFCI and FCI algorithms are shown in Figure 3(b) and (c), respectively. We see that the output of RFCI contains an extra edge, namely $X_1 \leftrightarrow X_5$.

As in Example 1, this edge is present after Step 1 of both algorithms. The reason is that the conditional independence $X_1 \perp\!\!\!\perp X_5 | \{X_2, X_3, X_4\}$ is not found, because $\{X_2, X_3, X_4\}$ is not a subset of $\text{adj}(\mathcal{C}_1, X_1)$ nor of $\text{adj}(\mathcal{C}_1, X_5)$, where \mathcal{C}_1 denotes the skeleton after Step 1.

The FCI algorithm finds this conditional independence in Step 3 when subsets of Possible-D-SEP are considered. The RFCI algorithm does not find this conditional independence, since the edge between X_1 and X_5 does not appear in an unshielded triple or a discriminating path. However, the ancestral information encoded by the output of RFCI is correct, and in this example identical to the ancestral information encoded by the output of FCI.

Finally, we show that the RFCI-PAG in Figure 3(b) describes two Markov equivalence classes. Consider a new DAG \mathcal{G}' , which is adapted from \mathcal{G} in Fig-

ure 3(a) by adding one additional latent variable L_3 pointing at X_1 and X_5 . This modification implies that X_1 and X_5 are conditionally dependent given any subset of the remaining observed variables, so that \mathcal{G}' belongs to a different Markov equivalence class than \mathcal{G} . The output of both FCI and RFCI, when using as input the conditional independence relationships that can be read off from \mathcal{G}' , is given in Figure 3(b). Hence, the PAG in Figure 3(b) represents more than one Markov equivalence class if interpreted as an RFCI-PAG.

3.4. *A class of graphs for which the outputs of FCI and RFCI are identical.* We now specify graphical conditions on an underlying DAG $\mathcal{G} = (\mathbf{V}, \mathbf{E})$ with $\mathbf{V} = \mathbf{X} \dot{\cup} \mathbf{L} \dot{\cup} \mathbf{S}$ such that the outputs of FCI and RFCI are identical (Theorem 3.3). Moreover, if the outputs of RFCI and FCI are not identical, we infer properties of edges that are present in the output of RFCI but not in that of FCI (Theorem 3.4).

The results in this section rely on the concept of inducing paths [21, 22], which we have extended here:

DEFINITION 3.5. Let $\mathcal{G} = (\mathbf{V}, \mathbf{E})$ be a DAG with $\mathbf{V} = \mathbf{X} \dot{\cup} \mathbf{L} \dot{\cup} \mathbf{S}$ and let \mathbf{Y} be a subset of \mathbf{X} containing X_i and X_j with $X_i \neq X_j$. A path π between X_i and X_j is called an *inducing path relative to \mathbf{Y} given \mathbf{S}* if and only if every member of $\mathbf{Y} \cup \mathbf{S}$ that is a nonendpoint on π is a collider on π and every collider on π has a descendant in $\{X_i, X_j\} \cup \mathbf{S}$.

We note that our Definition 3.5 corresponds to the one in [21] if $\mathbf{Y} = \mathbf{X}$. The existence of an inducing path in a DAG is related to d -connection in the following way. There is an inducing path between X_i and X_j relative to \mathbf{Y} given \mathbf{S} if and only if X_i and X_j are not d -separated by $(\mathbf{Y}' \cup \mathbf{S}) \setminus \{X_i, X_j\}$ for all $\mathbf{Y}' \subseteq \mathbf{Y}$ (see [21], Lemma 9, page 243). The definition of an inducing path is monotone in the following sense: if $\mathbf{Y}_1 \subseteq \mathbf{Y}_2 \subseteq \mathbf{X}$ and there is an inducing path between X_i and X_j relative to \mathbf{Y}_2 given \mathbf{S} , then there also is an inducing path between X_i and X_j relative to \mathbf{Y}_1 given \mathbf{S} .

Consider a pair of vertices $X_i, X_j \in \mathbf{X}$ in an underlying DAG \mathcal{G} . We introduce the following shorthand notation. Let $\text{Adj}(i, j) = \text{adj}(\mathcal{C}_1, X_i) \setminus \{X_j\}$, where \mathcal{C}_1 is the initial skeleton after Step 1 of the algorithms. Moreover, let $\text{Pds}(i, j) = \text{pds}(\mathcal{C}_2, X_i, X_j) \setminus \{X_j, X_i\}$, where \mathcal{C}_2 is the graph resulting from Step 2 of the FCI algorithm. By definition, $\text{Pds}(k, i) \supseteq \text{Adj}(k, i)$ for any pair of vertices $X_k, X_i \in \mathbf{X}$. We now consider the following three scenarios:

(S1) There is an inducing path between X_i and X_j in \mathcal{G} relative to $\text{Pds}(i, j)$ given \mathbf{S} , and there is an inducing path between X_i and X_j relative to $\text{Pds}(j, i)$ given \mathbf{S} .

(S2) There is an inducing path between X_i and X_j in \mathcal{G} relative to $\text{Adj}(i, j)$ given \mathbf{S} , and there is an inducing path between X_i and X_j relative to $\text{Adj}(j, i)$ given \mathbf{S} . Moreover, there is no inducing path between X_i and X_j

in \mathcal{G} relative to $\text{Pds}(i, j)$ given \mathbf{S} , or there is no inducing path between X_i and X_j in \mathcal{G} relative to $\text{Pds}(j, i)$ given \mathbf{S} .

(S3) There is no inducing path between X_i and X_j in \mathcal{G} relative to $\text{Adj}(i, j)$ given \mathbf{S} , or there is no inducing path between X_i and X_j in \mathcal{G} relative to $\text{Adj}(j, i)$ given \mathbf{S} .

We now obtain the following theorem:

THEOREM 3.3. *Assume that the distribution of $\mathbf{V} = \mathbf{X} \dot{\cup} \mathbf{L} \dot{\cup} \mathbf{S}$ is faithful to an underlying DAG \mathcal{G} . Then the output \mathcal{C}' of RFCI equals the output \mathcal{C}'' of FCI if for every pair of vertices X_i, X_j in \mathbf{X} either (S1) holds or (S3) holds. If $\mathcal{C}' \neq \mathcal{C}''$, then the skeleton of \mathcal{C}' is a strict superset of the skeleton of \mathcal{C}'' , and Scenario (S2) must hold for every pair of vertices that are adjacent in \mathcal{C}' but not in \mathcal{C}'' .*

Scenario (S2) occurs if and only if (i) there is a path $\pi(i, j)$ between X_i and X_j in the underlying DAG \mathcal{G} that satisfies: (c1) all colliders on $\pi(i, j)$ have descendants in $\{X_i, X_j\} \cup \mathbf{S}$, (c2) every member of $\text{Adj}(i, j) \cup \mathbf{S}$ on $\pi(i, j)$ is a collider on $\pi(i, j)$, (c3) there is a member of $(\text{Pds}(i, j) \cup \text{Pds}(j, i)) \setminus \text{Adj}(i, j)$ on $\pi(i, j)$ that is not a collider on the path, and (ii) there is a path $\pi(j, i)$ between X_j and X_i in the underlying DAG that satisfies conditions (c1)–(c3) above with the roles of i and j reversed. In condition (c3), an equivalent formulation is given by replacing $\text{Pds}(i, j) \cup \text{Pds}(j, i)$ with $\mathbf{X} \setminus \{X_i, X_j\}$.

To illustrate Theorem 3.3, consider again Example 2 and the graphs in Figure 3. The output of RFCI for the underlying DAG shown in Figure 3(a) contains an edge between X_1 and X_5 , while the output of FCI does not. According to Theorem 3.3, Scenario (S2) must hold for the vertices X_1 and X_5 . Hence, there must exist paths $\pi(1, 5)$ and $\pi(5, 1)$ between X_1 and X_5 in the underlying DAG that satisfy conditions (c1)–(c3) above. This is indeed the case for the path $\pi = \pi(1, 5) = \pi(5, 1) = \langle X_1, L_1, X_2, X_3, X_4, L_2, X_5 \rangle$: (c1) there are two colliders on π , X_2 and X_4 , both with descendants in $\{X_1, X_5\}$, (c2) all members of $\text{Adj}(1, 5) = \text{Adj}(5, 1) = \{X_2, X_4\}$ on π are colliders on the path, and (c3) X_3 is a member of $(\text{Pds}(1, 5) \cup \text{Pds}(5, 1)) \setminus \text{Adj}(1, 5) = (\text{Pds}(5, 1) \cup \text{Pds}(1, 5)) \setminus \text{Adj}(5, 1)$ on π and is a noncollider on π .

To see that the occurrence of Scenario (S2) does not always lead to a difference in the outputs of FCI and RFCI, we revisit Example 1 and the graphs in Figure 2. The same path π as above satisfies conditions (c1)–(c3) in the underlying DAG, but the outputs of FCI and RFCI are identical (due to the extra tests in Step 2 of Algorithm 3.2). This illustrates that fulfillment of (S1) or (S3) for every pair of vertices is not a necessary condition for equality of FCI and RFCI.

Finally, the following theorem establishes features of edges that are present in an RFCI-PAG but not in an FCI-PAG.

THEOREM 3.4. *Assume that the distribution of $\mathbf{V} = \mathbf{X} \dot{\cup} \mathbf{L} \dot{\cup} \mathbf{S}$ is faithful to an underlying DAG \mathcal{G} . If there is an edge $X_i \ast\ast X_j$ in an RFCI-PAG*

for \mathcal{G} that is not present in an FCI-PAG for \mathcal{G} , then the following hold:
 (i) $X_i \notin \text{an}(\mathcal{G}, X_j \cup \mathbf{S})$ and $X_j \notin \text{an}(\mathcal{G}, X_i \cup \mathbf{S})$, and (ii) each edge mark of $X_i \ast\ast X_j$ in the RFCI-PAG is a circle or an arrowhead.

4. Consistency of FCI and RFCI in sparse high-dimensional settings.

Let $\mathcal{G} = (\mathbf{V}, \mathbf{E})$ be a DAG with $\mathbf{V} = \mathbf{X} \dot{\cup} \mathbf{L} \dot{\cup} \mathbf{S}$ and let \mathcal{M} be the corresponding unique MAG over \mathbf{X} . We assume that we observe n i.i.d. copies of $\mathbf{W} = (W_1, \dots, W_p) \sim (X_1 | \mathbf{S}, \dots, X_p | \mathbf{S})$. To represent high-dimensional behavior, we let the DAG \mathcal{G} and the number of observed variables p in \mathbf{X} grow as a function of the sample size, so that $p = p_n$, $\mathcal{G} = \mathcal{G}_n$ and $\mathcal{M} = \mathcal{M}_n$. We do not impose any restrictions on the number of latent and selection variables. Throughout, we assume that \mathbf{W} is multivariate Gaussian, so that conditional independence is equivalent to zero partial correlation.

In Section 4.1, we define the sample versions of RFCI and the different versions of FCI. Sections 4.2 and 4.3 contain consistency results for RFCI and FCI in sparse high-dimensional settings. The conditions required for consistency of RFCI are considerably weaker than those for FCI.

4.1. *Sample versions of RFCI and the different versions of FCI.* Let $\rho_{n;i,j|\mathbf{Y}}$ be the partial correlation between W_i and W_j in \mathbf{W} given a set $\mathbf{Y} \subseteq \mathbf{W} \setminus \{W_i, W_j\}$, and let $\hat{\rho}_{n;i,j|\mathbf{Y}}$ be the corresponding sample partial correlation. We test if a partial correlation is equal to zero after applying Fisher's z-transform defined as $g(x) = \frac{1}{2} \log\left(\frac{1+x}{1-x}\right)$. Thus, we consider

$$\hat{z}_{n;i,j|\mathbf{Y}} = g(\hat{\rho}_{n;i,j|\mathbf{Y}}) \quad \text{and} \quad z_{n;i,j|\mathbf{Y}} = g(\rho_{n;i,j|\mathbf{Y}})$$

and we reject the null-hypothesis $H_0(i, j | \mathbf{Y}) : \rho_{i,j|\mathbf{Y}} = 0$ against the two-sided alternative $H_A(i, j | \mathbf{Y}) : \rho_{i,j|\mathbf{Y}} \neq 0$ at significance level α if

$$(4.1) \quad |\hat{z}_{n;i,j|\mathbf{Y}}| > \Phi^{-1}(1 - \alpha/2)(n - |\mathbf{Y}| - 3)^{-1/2},$$

where $\Phi(\cdot)$ denotes the cumulative distribution function of a standard normal random variable. (We assume $n > |\mathbf{Y}| + 3$.)

Sample versions of RFCI and the different versions of FCI can be obtained by simply adapting all steps with conditional independence decisions as follows: X_i and X_j are judged to be conditionally independent given $\mathbf{Y}' \cup \mathbf{S}$ for $\mathbf{Y}' \subseteq \mathbf{X} \setminus \{X_i, X_j\}$ if and only if $|\hat{z}_{n;i,j|\mathbf{Y}}| \leq \Phi^{-1}(1 - \alpha/2)(n - |\mathbf{Y}'| - 3)^{-1/2}$ for $\mathbf{Y} \sim \mathbf{Y}' | \mathbf{S}$. The parameter α is used for many tests, and plays the role of a tuning parameter.

4.2. *Consistency of RFCI.* We impose the following assumptions:

(A1) The distribution of \mathbf{W} is faithful to the underlying causal MAG \mathcal{M}_n for all n .

(A2) The number of variables in \mathbf{X} , denoted by p_n , satisfies $p_n = O(n^a)$ for some $0 \leq a < \infty$.

(A3) The maximum size of the adjacency sets after Step 1 of the oracle RFCI algorithm, denoted by $q_n = \max_{1 \leq i \leq p_n} (|\text{adj}(\mathcal{C}_1, X_i)|)$, where \mathcal{C}_1 is the skeleton after Step 1, satisfies $q_n = O(n^{1-b})$ for some $0 < b \leq 1$.

(A4) The distribution of \mathbf{W} is multivariate Gaussian.

(A5) The partial correlations satisfy the following lower and upper bound for all $W_i, W_j \in \{W_1, \dots, W_{p_n}\}$ and $\mathbf{Y} \subseteq \{W_1, \dots, W_{p_n}\} \setminus \{W_i, W_j\}$ with $|\mathbf{Y}| \leq q_n$:

$$\begin{aligned} \inf\{|\rho_{n;i,j|\mathbf{Y}}| : \rho_{n;i,j|\mathbf{Y}} \neq 0\} &\geq c_n, \\ \sup\{|\rho_{n;i,j|\mathbf{Y}}| : i \neq j\} &\leq M < 1, \end{aligned}$$

where $c_n^{-1} = O(n^d)$ for some $0 \leq d < b/2$ with b from (A3).

Assumption (A2) allows the number of variables to grow as any polynomial of the sample size, representing a high-dimensional setting. Assumption (A3) is a sparseness assumption, and poses a bound on the growth of the maximum size of the adjacency sets in the graph resulting from Step 1 of the oracle RFCI algorithm. The upper bound in assumption (A5) excludes sequences of models in which the partial correlations tend to 1, hence avoiding identifiability problems. The lower bound in assumption (A5) requires the nonzero partial correlations to be outside of the $n^{-b/2}$ range, with b as in assumption (A3). This condition is similar to assumption 5 in [12] and condition (8) in [25].

The similarities between our assumptions and the assumptions of [8] for consistency of the PC algorithm are evident. The main differences are that our assumption (A3) concerns the skeleton after Step 1 of the oracle RFCI algorithm instead of the underlying DAG, and that our assumptions (A1) and (A4)–(A5) concern the distribution of \mathbf{W} instead of \mathbf{X} .

THEOREM 4.1. *Assume (A1)–(A5). Denote by $\hat{\mathcal{C}}_n(\alpha_n)$ the output of the sample version of the RFCI algorithm and by \mathcal{C}'_n the oracle version of the RFCI algorithm. Then there exists a sequence $\alpha_n \rightarrow 0$ ($n \rightarrow \infty$) and a constant $0 < C < \infty$ such that*

$$\mathbb{P}[\hat{\mathcal{C}}_n(\alpha_n) = \mathcal{C}'_n] \geq 1 - O(\exp(-Cn^{1-2d})) \rightarrow 1 \quad \text{as } n \rightarrow \infty,$$

where $d > 0$ is as in (A5).

One such sequence for α_n is $\alpha_n = 2(1 - \Phi(n^{1/2}c_n/2))$, where c_n is the lower bound in (A5) (which depends on the unknown data distribution).

4.3. Consistency of FCI. Assume (A1)–(A5) of Section 4.2, but replace (A3) by (A3'):

(A3') The maximum size of the Possible-D-SEP sets in Step 3 of the oracle FCI algorithm, denoted by $r_n = \max_{1 \leq i \leq p_n} (|\text{pds}(\mathcal{C}_2, X_i, \cdot)|)$, where \mathcal{C}_2 is the graph resulting from Step 2, satisfies $r_n = O(n^{1-b})$ for some $0 < b \leq 1$.

Assumption (A3') is stronger than assumption (A3), since the skeleton after Step 1 of the RFCI algorithm is identical to the skeleton after Step 2 of the FCI algorithm, and since the adjacency set is contained in Possible-D-SEP by definition. (In fact, one can construct sequences of graphs in which the maximum size of the adjacency sets is fixed, but the maximum size of the Possible-D-SEP sets grows linearly with the number of vertices.) The stricter assumption (A3') is needed for the additional conditional independence tests in Step 3 of the FCI algorithm.

THEOREM 4.2. *Assume (A1)–(A5) with (A3') instead of (A3). Consider one of the sample versions of FCI, FCI_{path} , CFCI, $CFCI_{\text{path}}$, SCFCI or $SCFCI_{\text{path}}$, and denote its output by $\mathcal{C}_n^*(\alpha_n)$. Denote the true underlying FCI-PAG by \mathcal{C}_n . Then there exists a sequence $\alpha_n \rightarrow 0$ ($n \rightarrow \infty$) and a constant $0 < C < \infty$ such that*

$$\mathbb{P}[\mathcal{C}_n^*(\alpha_n) = \mathcal{C}_n] \geq 1 - O(\exp(-Cn^{1-2d})) \rightarrow 1 \quad \text{as } n \rightarrow \infty,$$

where $d > 0$ is as in (A5).

As before, one such sequence for α_n is $\alpha_n = 2(1 - \Phi(n^{1/2}c_n/2))$, where c_n is the lower bound in (A5).

5. Numerical examples. In this section we compare the performance of RFCI and different versions of FCI and Anytime FCI in simulation studies, considering both the computing time and the estimation performance. Since Anytime FCI requires an additional tuning parameter (see [19] and Section 3 of [5]), we cannot compare it directly. We therefore define a slight modification, called Adaptive Anytime FCI (AAFCI), where this tuning parameter is set adaptively (see Section 3 of [5]). Our proposed modifications of FCI (see Section 3.1) can also be applied to AAFCI, leading to the following algorithms: $AAFCI_{\text{path}}$, $CAAFCI$, $CAAFCI_{\text{path}}$, $SCAAFCI$ and $SCAAFCI_{\text{path}}$.

The remainder of this section is organized as follows. The simulation setup is described in Section 5.1. Section 5.2 shows that the estimation performances of RFCI and all versions of FCI and AAFCI are very similar. Section 5.3 shows that our adaptations of FCI and AAFCI can reduce the computation time significantly for graphs of moderate size, but that RFCI is the only feasible algorithm for large graphs.

5.1. Simulation setup. We use the following procedure to generate a random DAG with a given number of vertices p' and expected neighborhood size $E(N)$. First, we generate a random adjacency matrix A with independent realizations of Bernoulli($E(N)/(p' - 1)$) random variables in the lower triangle of the matrix and zeroes in the remaining entries. Next, we replace

the ones in A by independent realizations of a $\text{Uniform}([0.1, 1])$ random variable. A nonzero entry A_{ij} can be interpreted as an edge from X_j to X_i with “strength” A_{ij} , in the sense that $X_1, \dots, X_{p'}$ can be generated as follows: $X_1 = \varepsilon_1$ and $X_i = \sum_{r=1}^{i-1} A_{ir} X_r + \varepsilon_i$ for $i = 2, \dots, p'$, where $\varepsilon_1, \dots, \varepsilon_{p'}$ are mutually independent $\mathcal{N}(0, 1)$ random variables. The variables $X_1, \dots, X_{p'}$ then have a multivariate Gaussian distribution with mean zero and covariance matrix $\Sigma' = (\mathbb{1} - A)^{-1}(\mathbb{1} - A)^{-T}$, where $\mathbb{1}$ is the $p' \times p'$ identity matrix.

To assess the impact of latent variables, we randomly define half of the variables that have no parents and at least two children to be latent (we do not consider selection variables). We restrict ourselves to variables that have no parents and at least two children, since these are particularly difficult for RFCI in the sense that they are likely to satisfy Scenario (S2) in Section 3.4. Throughout, we let p denote the number of observed variables.

We consider the oracle versions of RFCI and FCI_{path} (note that the outputs of FCI_{path} and FCI are identical in the oracle versions), and the sample versions of RFCI, (AA)FCI, (AA) FCI_{path} , C(AA)FCI, C(AA) FCI_{path} and SC(AA) FCI_{path} . In all plots (AA) FCI_{path} is abbreviated as (AA)FCIp. Let Σ be the $p \times p$ matrix that is obtained from Σ' by deleting the rows and columns that correspond to latent variables. The oracle versions of the algorithms use Σ as input, and the sample versions of the algorithms use simulated data from a $N_p(0, \Sigma)$ distribution as input.

The simulations were performed on an AMD Opteron (tm) Quad Core Processor 8380 with 2.5 GHz and 2 GB RAM on Linux using R 2.11.0.

5.2. Estimation performance. We first investigated the difference between the oracle versions of RFCI and FCI_{path} , using simulation settings $p' \in \{15, 20, 25\}$ and $E(N) = 2$. For each combination of these parameters, we generated 1000 DAGs, where the average number of observed variables was $p \approx \{14, 18, 23\}$ (rounded to the nearest integer). For each simulated graph, we assessed whether the outputs of FCI_{path} and RFCI were different, and if this was the case, we counted the number of additional edges in the output of RFCI when compared to that of FCI. For $p' = 15$, $p' = 20$ and $p' = 25$, there were 0, 1 and 5 of the 1000 DAGs that gave different results, and whenever there was a difference, the output of RFCI had a single additional edge. Hence, for these simulation settings, the oracle versions of FCI_{path} and RFCI were almost always identical, and if there was a difference, the difference was very small.

Next, we investigated the performance of the sample versions of RFCI and our adaptations of FCI and AAFCI, considering the number of differences in the output when compared to the true FCI-PAG. We used two simulation settings: small-scale and large-scale.

The small-scale simulation setting is as follows. For each value of $p' \in \{10, 15, 20, 25, 30\}$, we generated 50 random DAGs with $E(N) = 2$, where

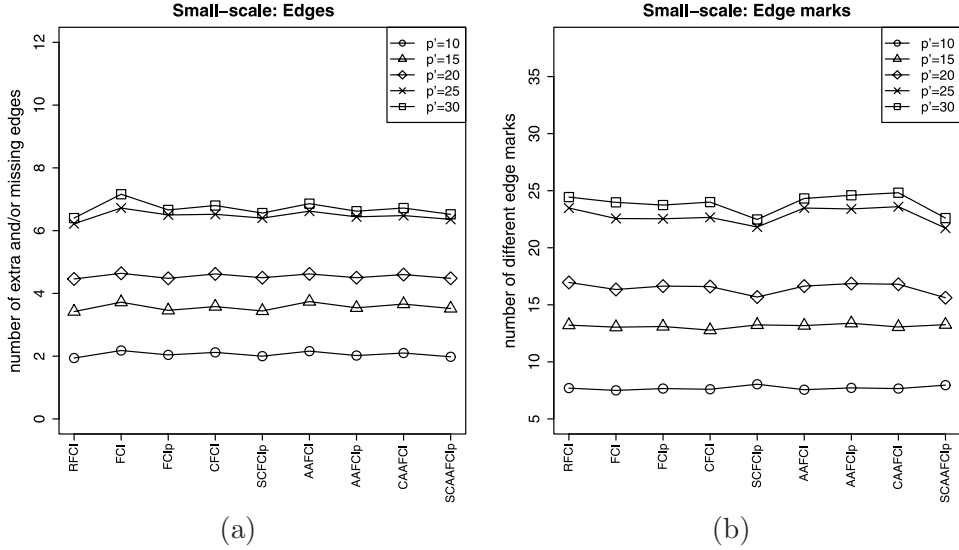


FIG. 4. Estimation performance of the sample versions of RFCI and the different versions of FCI and AAFCI in the small-scale setting, when compared to the true underlying FCI-PAG. The simulation settings were $E(N) = 2$, $n = 1000$ and $\alpha = 0.01$. (a) Average number of missing or extra edges over 50 replicates; (b) average number of different edge marks over 50 replicates.

the average number of observed variables was $p \approx \{9, 14, 18, 23, 27\}$. For each such DAG, we generated a data set of size $n = 1000$ and ran RFCI, (AA)FCI, (AA)FCI_{path}, C(AA)FCI and SC(AA)FCI_{path} with tuning parameter $\alpha = 0.01$.

Figure 4 shows the results for the small-scale setting. Figure 4(a) shows the average number of missing or extra edges over the 50 replicates, and we see that this number was virtually identical for all algorithms. Figure 4(b) shows the average number of different edge marks over the 50 replicates. We again see that all algorithms performed similarly. We note that the conservative and superconservative adaptations of the algorithms yield slightly better edge orientations than the standard versions for larger graphs.

The large-scale simulation setting is as follows. For each value of $p' \in \{100, 200, 300, 500\}$ we generated 100 random DAGs with $E(N) = 3$, where the average number of observed variables was $p \approx \{90, 180, 271, 452\}$. For each DAG, we generated a data set of size $n = 1000$, and ran RFCI, CFci_{path} and CAAFCI_{path} [the other versions of (AA)FCI were computationally infeasible] using tuning parameter $\alpha = 0.01$. To ensure reasonable computing times, we terminated an algorithm for a graph if it was not finished after eight hours. For CFci_{path}, termination occurred five times for $p' = 300$ and nine times for $p' = 500$. One of the latter nine graphs also led to termination of CAAFCI_{path}. To ensure comparability we deleted any run which did not

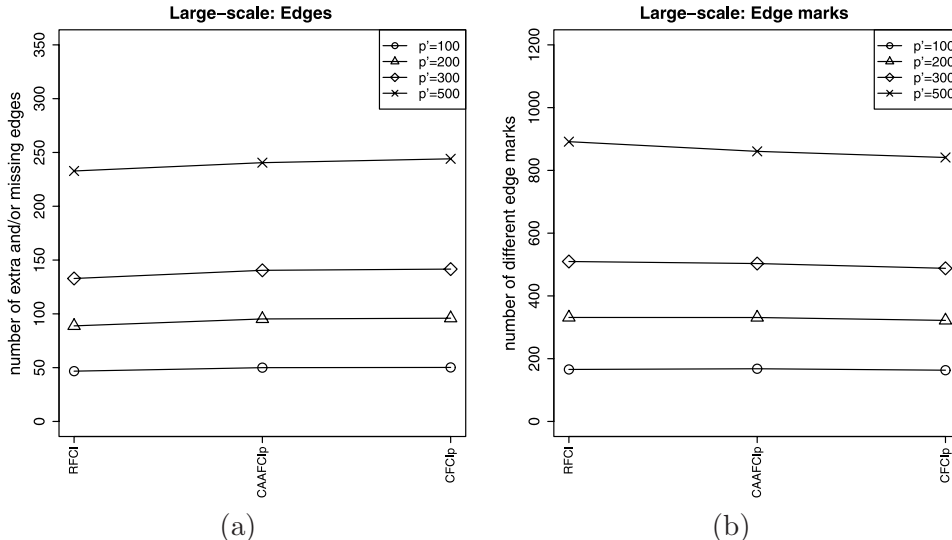


FIG. 5. Estimation performance of the sample versions of RFCI and the fastest versions of FCI and AAFCI in the large-scale setting, when compared to the true underlying FCI-PAG. The simulation settings were $E(N) = 3$, $n = 1000$ and $\alpha = 0.01$. (a) Average number of missing or extra edges over 91 replicates (see text); (b) average number of different edge marks over 91 replicates (see text).

complete for all algorithms and computed the average number of missing or extra edges [see Figure 5(a)] and the average number of different edge marks [see Figure 5(b)] over the 91 remaining runs. We again see that all algorithms performed similarly.

5.3. *Computing time.* We first compared the size of the Possible-D-SEP sets in the different versions of FCI, since this is the most important factor for the computing time of these algorithms. In particular, if the size of Possible-D-SEP is, say, 25 vertices or more, it becomes computationally infeasible to consider all of its subsets. For all combinations of $p' \in \{10, 50, 250\}$ and $E(N) \in \{2, 3\}$, we generated 100 random graphs and ran the oracle version of FCI and FCI_{path} and the sample versions of FCI, FCI_{path} , CFClp and $\text{CFClp}_{\text{path}}$. The average number of observed variables was $p \approx \{9, 46, 230\}$ for $E(N) = 2$ and $p \approx \{9, 45, 226\}$ for $E(N) = 3$. For the sample versions of the algorithms we used sample size $n = 1000$ and tuning parameter $\alpha = 0.01$. For each simulated graph and each algorithm we computed the maximum size of the Possible-D-SEP sets over all vertices in the graph. We averaged these numbers over the 100 replicates, and denoted the result by mean-max-pds. The results are shown in Figure 6. We see that the new definition of pds_{path} (see Definition 3.4 used in algorithm FCI_{path} and $\text{CFClp}_{\text{path}}$) reduced mean-max-pds slightly, while the conservative adaptations of the sample versions of the algorithms reduced it drastically. These results are also relevant for the

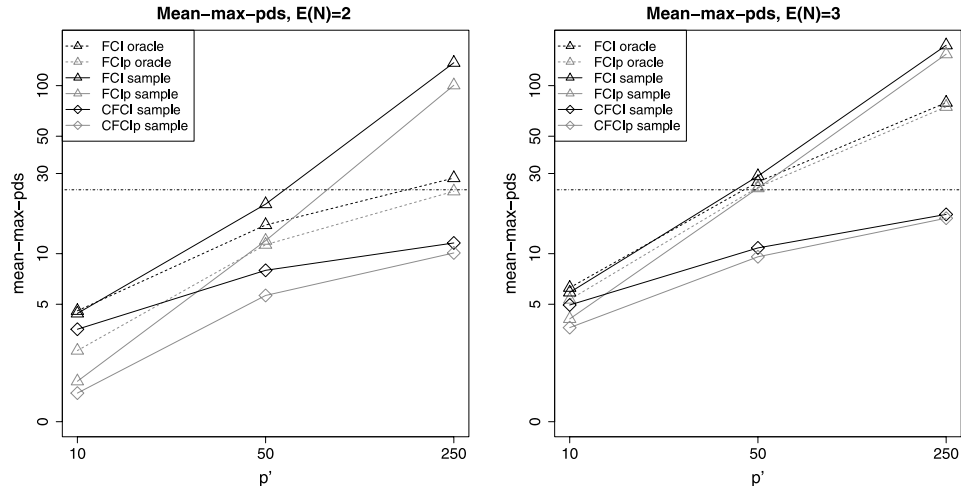


FIG. 6. A plot of *mean-max-pds* (see text) versus p' , where both axes are drawn in log scale. The horizontal line at *mean-max-pds* = 24 indicates an upper bound that still yields a feasible running time of the algorithms.

different versions of AAFCI, since AAFCI considers all subsets of Possible D-SEP up to a certain size. This again becomes infeasible if Possible D-SEP is large.

Next, we investigated the computing time of the sample version of RFCI and modifications of FCI and AAFCI under the same simulation settings as in Section 5.2.

Figure 7(a) shows the average running times over the 50 replicates in the small-scale setting. We see that RFCI was fastest for all parameter settings, while the standard version of FCI was slowest for all settings with $p' \geq 15$. Our new adaptations of FCI and AAFCI reduced the running time of FCI and AAFCI significantly, which is in correspondence with the reduction in *mean-max-pds* that we saw in Figure 6.

Figure 7(b) shows the average running times over the 91 fastest runs in the large-scale setting. We see that RFCI is the only algorithm that is computationally feasible for large graphs: for $p' = 500$ RFCI took about 40 seconds, while the fastest modifications of FCI took about 10,000 seconds. These results can be explained by the fact that Steps 2 and 3 in the RFCI algorithm only involve local tests (conditioning on subsets of the adjacency set of a vertex), while Step 3 of (AA)FCI considers subsets of the Possible D-SEP sets, which can be large even for sparse graphs (see Figure 6).

6. Discussion. In this paper, we introduce a new algorithm for learning PAGs, called the Really Fast Causal Inference (RFCI) algorithm. RFCI uses fewer conditional independence tests than the existing FCI algorithm, and its tests condition on a smaller number of variables.

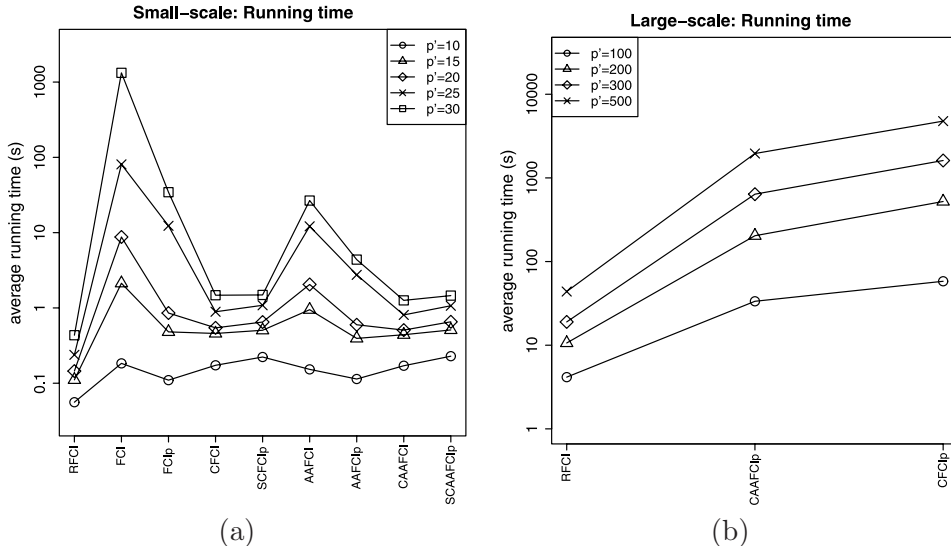


FIG. 7. Running time of the sample versions of the algorithms, using simulation settings $n = 1000$ and $\alpha = 0.01$, where the y-axes are drawn in log scale. (a) Average running time in seconds of each algorithm over 50 replicates, using $E(N) = 2$; (b) average running time in seconds of each algorithm over 91 replicates (see text), using $E(N) = 3$.

The output of RFCI can be interpreted as the output of FCI, with the only difference that the presence of an edge has a weaker meaning. In particular, the interpretation of tails and arrowheads is identical for both algorithms. In this sense the RFCI algorithm is similar to the Anytime FCI algorithm of [19].

We describe a class of graphs where the outputs of FCI and RFCI are identical, and show that differences between the two algorithms are caused by very special structures in the underlying DAG. We confirm this finding in simulation studies that show that differences between the oracle versions of RFCI and FCI are very rare.

We prove consistency of FCI and RFCI in sparse high-dimensional settings. The sparsity conditions needed for consistency of RFCI are considerably weaker than those needed for FCI, due to the lower computational complexity of the RFCI algorithm.

We compare RFCI with several modifications of (Anytime) FCI in simulation studies. We show that all algorithms perform similarly in terms of estimation, and that RFCI is the only algorithm that is computationally feasible for high-dimensional sparse graphs.

We envision several possible uses of RFCI. First, it could be used in addition to the PC algorithm to assess the potential impact of the existence of latent or selection variables. Second, it could be used as a building block

for an IDA-like method [10, 11] to obtain bounds on causal effects based on observational data that is faithful to an *unknown* underlying causal graph *with arbitrarily many latent and selection variables*. In order to achieve the latter, we plan to build on the work of [17, 23], who made a start with the study of causal reasoning for ancestral graphs. Other interesting open problems include investigating which RFCI-PAGs can only correspond to a single Markov equivalence class, and investigating completeness of the RFCI algorithm, that is, investigating whether the edge marks in the output of RFCI are maximally informative.

SUPPLEMENTARY MATERIAL

Supplement to “Learning high-dimensional directed acyclic graphs with latent and selection variables” (DOI: [10.1214/11-AOS940SUPP](https://doi.org/10.1214/11-AOS940SUPP); .pdf). All proofs, a description of the Adaptive Anytime FCI algorithm, pseudocodes, and two additional examples can be found in the supplementary document [5].

REFERENCES

- [1] AHO, A., HOPCROFT, J. and ULLMAN, J. D. (1974). *The Design and Analysis of Computer Algorithms*. Addison-Wesley, Boston, MA.
- [2] ALI, R. A., RICHARDSON, T. S. and SPIRITES, P. (2009). Markov equivalence for ancestral graphs. *Ann. Statist.* **37** 2808–2837. [MR2541448](#)
- [3] ANDERSSON, S. A., MADIGAN, D. and PERLMAN, M. D. (1997). A characterization of Markov equivalence classes for acyclic digraphs. *Ann. Statist.* **25** 505–541. [MR1439312](#)
- [4] CHICKERING, D. M. (2002). Learning equivalence classes of Bayesian-network structures. *J. Mach. Learn. Res.* **2** 445–498. [MR1929415](#)
- [5] COLOMBO, D., MAATHUIS, M. H., KALISCH, M. and RICHARDSON, T. S. (2012). Supplement to “Learning high-dimensional directed acyclic graphs with latent and selection variables.” DOI:[10.1214/11-AOS940SUPP](https://doi.org/10.1214/11-AOS940SUPP).
- [6] COOPER, G. (1995). Causal discovery from data in the presence of selection bias. In *Preliminary Papers of the Fifth International Workshop on Artificial Intelligence and Statistics* (D. FISHER, ed.) 140–150.
- [7] DAWID, A. P. (1980). Conditional independence for statistical operations. *Ann. Statist.* **8** 598–617. [MR0568723](#)
- [8] KALISCH, M. and BÜHLMANN, P. (2007). Estimating high-dimensional directed acyclic graphs with the PC-algorithm. *J. Mach. Learn. Res.* **8** 613–636.
- [9] KALISCH, M., MÄCHLER, M., COLOMBO, D., MAATHUIS, M. H. and BÜHLMANN, P. (2012). Causal inference using graphical models with the R package pcalg. *J. Statist. Software*. To appear.
- [10] MAATHUIS, M. H., COLOMBO, D., KALISCH, M. and BÜHLMANN, P. (2010). Predicting causal effects in large-scale systems from observational data. *Nat. Methods* **7** 247–248.
- [11] MAATHUIS, M. H., KALISCH, M. and BÜHLMANN, P. (2009). Estimating high-dimensional intervention effects from observational data. *Ann. Statist.* **37** 3133–3164. [MR2549555](#)

- [12] MEINSHAUSEN, N. and BÜHLMANN, P. (2006). High-dimensional graphs and variable selection with the lasso. *Ann. Statist.* **34** 1436–1462. [MR2278363](#)
- [13] PEARL, J. (2000). *Causality. Models, Reasoning, and Inference*. Cambridge Univ. Press, Cambridge. [MR1744773](#)
- [14] PEARL, J. (2009). Causal inference in statistics: An overview. *Stat. Surv.* **3** 96–146. [MR2545291](#)
- [15] RAMSEY, J., ZHANG, J. and SPIRITES, P. (2006). Adjacency-faithfulness and conservative causal inference. In *Proceedings of the 22nd Annual Conference on Uncertainty in Artificial Intelligence*. AUAI Press, Arlington, VA.
- [16] RICHARDSON, T. and SPIRITES, P. (2002). Ancestral graph Markov models. *Ann. Statist.* **30** 962–1030. [MR1926166](#)
- [17] RICHARDSON, T. S. and SPIRITES, P. (2003). Causal inference via ancestral graph models. In *Highly Structured Stochastic Systems. Oxford Statistical Science Series* **27** 83–113. Oxford Univ. Press, Oxford. [MR2082407](#)
- [18] ROBINS, J. M., HERNÁN, M. A. and BRUMBACK, B. (2000). Marginal structural models and causal inference in epidemiology. *Epidemiology* **11** 550–560.
- [19] SPIRITES, P. (2001). An anytime algorithm for causal inference. In *Proc. of the Eighth International Workshop on Artificial Intelligence and Statistics* 213–221. Morgan Kaufmann, San Francisco.
- [20] SPIRITES, P., GLYMOUR, C. and SCHEINES, R. (2000). *Causation, Prediction, and Search*, 2nd ed. MIT Press, Cambridge, MA. [MR1815675](#)
- [21] SPIRITES, P., MEEK, C. and RICHARDSON, T. (1999). An algorithm for causal inference in the presence of latent variables and selection bias. In *Computation, Causation, and Discovery* 211–252. AAAI Press, Menlo Park, CA. [MR1689972](#)
- [22] VERMA, T. and PEARL, J. (1990). Equivalence and synthesis of causal models. In *Proceedings of the Sixth Annual Conference on Uncertainty in Artificial Intelligence* 255–270. Elsevier, New York.
- [23] ZHANG, J. (2008). Causal reasoning with ancestral graphs. *J. Mach. Learn. Res.* **9** 1437–1474. [MR2426048](#)
- [24] ZHANG, J. (2008). On the completeness of orientation rules for causal discovery in the presence of latent confounders and selection bias. *Artificial Intelligence* **172** 1873–1896. [MR2459793](#)
- [25] ZHAO, P. and YU, B. (2006). On model selection consistency of Lasso. *J. Mach. Learn. Res.* **7** 2541–2563. [MR2274449](#)

D. COLOMBO
M. H. MAATHUIS
M. KALISCH
ETH ZÜRICH
SEMINAR FOR STATISTICS
RÄMISTRASSE 101
8092 ZÜRICH
SWITZERLAND
E-MAIL: colombo@stat.math.ethz.ch
maathuis@stat.math.ethz.ch
kalisch@stat.math.ethz.ch

T. S. RICHARDSON
DEPARTMENT OF STATISTICS
UNIVERSITY OF WASHINGTON
SEATTLE, WASHINGTON 98195
USA
E-MAIL: thomasr@u.washington.edu